Investigation of Cross-Coupling in Piezoelectric Transducer Arrays and Correction

Abdelmajid Bybi[1,*] Sébastien Grondel[2], Ahmed Mzerd[3], Christian Granger[4], Mohammed Garoum[1], Jamal Assaad[2]

[1]Mohammed V University in Rabat, High School of Technology in Sale, MEAT, Sale, Morocco
[2]Polytechnic University (UPHF), IEMN, UMR CNRS 8520, OAE Department, Valenciennes, France
[3]Mohammed V University in Rabat, Faculty of Science, STCE, Energy Research Center, Rabat, Morocco
[4]ISEN Department, IEMN, UMR CNRS 8520, Lille, France

Received 04 May 2019; received in revised form 02 June 2019; accepted 04 July 2019

Abstract

Cross-coupling in piezoelectric transducer arrays is an undesirable phenomenon which decreases the performance of these devices. Indeed, when one element of a transducer is driven, it generates parasitic displacement fields at the radiating surfaces of the neighboring elements, which changes the directivity of the array. The objective of this paper is to investigate the cross-coupling effects on the piezoelectric transducer arrays performance and to propose solutions to reduce this parasitic phenomenon. In this context, it is demonstrated that a filling material having high mechanical losses contributes to the reduction of cross-coupling. In addition to this, a procedure of active cancellation of cross-coupling is successfully tested in the case of two transducer arrays vibrating in the transverse mode for the first prototype and thickness mode for the second one. Finally, the ability of the method is demonstrated even when the displacement at the radiating surface of the transducer array is not uniform.

Keywords: cross-coupling, piezoelectric transducer arrays, correction method

1. Introduction

Linear and phased piezoelectric transducer arrays are usually employed in medical imaging and NDT applications. The major purpose of ongoing and future researches in this area is to optimize the electroacoustic performance of ultrasonic transducers in order to obtain a high image resolution for more reliable and safe diagnostics. These efforts include the use of specific materials instead of the traditional piezoelectric ceramics, like single crystals LiNbO3, PMN-PT and PIMNT [1-4]. Piezo-composite materials [5-7] have also been proposed for high-frequency applications (≥ 20 MHz) such as ophthalmology, dermatology, and small animals. Similarly, silicon micro-machined transducers [8-9] have been developed to replace conventional piezo-ceramic arrays and electronic devices could thus be integrated on the same substrate. Nevertheless, cross-coupling which is associated with acoustic wave propagation between successive array elements is a problem for all these kinds of arrays as it is responsible for anomalous behavior in the directivity of the array. In order to understand this phenomenon, many researchers have studied the origins and effects of cross-coupling in transducer arrays by using numerical [10-13] and experimental methods [14-16]. Recently, Pyo and Roh [17] developed a simple equivalent circuit inspired by Masons' model to analyze cross-coupling in an underwater planar array. In this study, a Tonpliz transducer is used as a

* Corresponding author. E-mail address: abdelmajid_bybi@hotmail.fr
Tel.: +212-6-39668291; Fax: +212-5-37881564

projector and its neighboring bar elements as hydrophones. The elements are connected to each other by only an acoustic window (water), i.e. the spaces between elements are empty and the matching layers not considered. Consequently, the direct cross-coupling between elements is not considered.

In literature research works devoted to the minimization of cross-coupling can be divided into three approaches. The first one investigates the contribution of the passive elements (filling material, matching layers, and backing) to the mechanical cross-coupling. The second solution consists in developing a systematic method for active cancellation of cross-coupling. The last method concerns specific treatments realized on the excitation and reception signals in order to reduce cross-coupling. In the first case, research works are dedicated particularly to the optimization of the filling material properties as an alternative to minimize mechanical cross-coupling. Branca et al. [18] proposed an empirical method based on the test of different filling materials utilized to manufacture eight transducer arrays. In this study, the choice of the suitable filling material is based on vibration measurements realized for each transducer array. The optimal filling material gave a reduction of cross-coupling about -10 dB in a PZT linear array. On the other hand, Lee and Roh [19] tested and optimized three structural variables such as the thickness of the matching layers, the width, and depth of the major and minor kerfs. The optimal structural variable gave a cross-coupling level -4.49 dB lower than that obtained in the literature. Concerning the optimization of the front matching layers, recent studies propose one or more layers with adequate acoustic impedances and a very low acoustic attenuation factor (<10 dB at the resonant frequency) [20]. Research works are also dedicated to the optimization of the back matching layer (backing) by choosing materials with acoustic impedance very close to that of the active element and having a high acoustic attenuation factor (e.g. porous ceramics) [21-22]. Recently, Hennenberg et al. proposed another alternative to reduce the mechanical cross-coupling through the backing by using a stop band material [23]. The proposed prototype is composed of a common backing with two bending elements (active and passive elements) bonded on top. In this case, the cross-coupling reduction is achieved by attaching local resonators on the downside of the backing. The optimal structure (backing with resonators having a length 9.4 mm) allowed the reduction of cross-coupling from -10.1 dB to -18 dB. Finally, in order to reduce cross-coupling due to the Printed Circuit Board (PCB) utilized to connect the transducer array elements, Celmer et al. [13] proposed some changes in the connection of electrodes and perforation of the elements of the PCB supporting elementary transducers. These studies contributed to the development of an enhanced version of ring arrays, where parasitic pulses caused by the electrical and mechanical cross-coupling are significantly reduced [15]. Concerning the second approach, previous studies [16, 24-25] provided a Finite Elements algorithm to adapt harmonic electrical voltages on each neighboring element of the active one in order to reduce the displacement field on their active surface. This method requires displacement measurements using a laser vibrometer or electrical measurements (impedance and current measurements). In the same context, Zhou et al. [26] developed another method using the transfer function matrix relating input voltages Vi to output pressures Pi in the case of transient excitations. In this case, the measurement precision of the elements' transfer function using a hydrophone, or other methods such as direct receive transfer measurement or pulse-echo technique [27], is limited. Therefore, the method is based on the transfer function calculated by FE, which is not perfectly matched to the real physical device. Finally, according to the last approach, an interesting solution concerns the processing of the digital signal obtained at the output of the acquisition chain by applying an adaptive filter to the noisy signal. Nguyen et al. [28] proposed a signal processing method based on the use of an adaptive cross-coupling filter using the Radon transform. The simulation and experiment results have shown the effectiveness of this adaptive filter to eliminate the noise due to cross-coupling. Ishihara et al. [29] proposed another solution combining techniques of spatially coded excitation and synthetic aperture to suppress cross-coupling artifacts in higher-frame-rate ultrasound imaging. The efficiency of the method is evaluated numerically assuming phased array scanning. In, this case, a satisfactory reduction of cross-coupling is obtained, i.e. from -37 dB to less than -57 dB.

The aim of this paper is first, to highlight the cross-coupling effects in piezoelectric transducer arrays, numerically using 2D and 3D Finite Elements Models (FEM) and experimentally by electrical impedance and displacement measurements. It

studies particularly the effects of the mechanical cross-coupling due to the filling material and points out the influence of the material losses. Secondly, since the correction method previously proposed in [16, 24] was performed only on transducer arrays vibrating in thickness mode, and by considering a plane strain approximation (uniform displacement along the length of the transducer array), our purpose is to test the validity of the correction method in the case of two transducer arrays vibrating in thickness and transverse modes. Concerning the transducer array vibrating in thickness mode (seven-element array), the piezoelectric elements are polarized in the thickness direction and the vibration is also obtained in the same direction [30-31]. Whereas, in the case of the transducer array vibrating in transverse mode (five-element array), the elements are polarized along with their thickness but the vibration is mainly obtained in the orthogonal direction (along the width of the element W) [32-33]. Finally, the objective of this study is also to demonstrate the ability of the correction method to reduce cross-coupling even when the displacement at the radiating surface of the transducer array is not uniform.

The first section of this paper describes briefly the cross-coupling correction method and presents the fabricated prototypes. In the second section, numerical studies of cross-coupling are carried out in order to point out the influence of the mechanical losses of the filling material on the cross-coupling phenomenon and to test the correction method by using 2D and 3D FEM. The last section is dedicated to the application of the correction method to two fabricated transducer arrays: five-element array vibrating in transverse mode and seven-element array vibrating in thickness mode. All the calculations are carried out at low frequency in order to compare them with the experimental results, thus facilitating the fabrication of the transducer arrays.

2. General Description

2.1. Summary of the cross-coupling correction method

The method of active cancellation of cross-coupling is already described in details in [16, 24], only the main equations and assumptions are briefly recalled here. The ultrasonic transducer arrays usually consist of even number of elementary transducers and that number is the power of 2. This is related to digital channel control. In order to get a full symmetry of the array and to simplify calculations and analysis, an odd number of transducers is assumed (2N-1 elements). Furthermore, each element of the transducer array is considered operating independently and that the energy radiated is derived from the linear summation of the energy contribution of each element. If the problem of cross-coupling due to the electrical excitation of each element can be solved, the required excitations and their associated cross-coupling cancellation signals can be superimposed to achieve the required beamforming effect. The beamforming task can, therefore, be separated from the cross-coupling task. Following the previous reasoning, it is possible to consider that the normal displacement of the i^{th} element u_i when all array elements are electrically excited can be decomposed as the sum of the displacements due to each electrical excitation. It yields to:

$$u_i = \sum_{j=1}^{2N-1} u_i^j \tag{1}$$

where u_i^j corresponds to the normal displacement of the i^{th} element when an electrical voltage of 1V is applied to the j^{th} one.

Indeed, since a linear relationship exists between the electrical voltage applied to each element and the resulting displacements, it is possible to reduce the cross-coupling due to the excitation of the kth element by solving the following system:

$$u_i(\text{corrected}) = \sum_{j=1, j\neq k}^{2N-1} A_j^k \, u_i^j + u_i^k \quad \begin{matrix} =0 & \forall i \neq k \\ \neq & \text{for } i=k \end{matrix} \tag{2}$$

where A_j^k represent the electrical voltages (the unknowns of the problem) to apply to the neighboring elements of the k^{th} element in order to cancel the parasitic displacements.

In the case of a harmonic excitation, the displacement u_i^j can be expressed in the following form:

$$u_i^j = C_i^j e^{j\omega t} \tag{3}$$

where C_i^k is a complex value considering the modulus and the phase of the displacement. Consequently, the resolution of the Eq. (2) leads to complex values of the electrical voltages A_j^k.

2.2. Fabricated prototypes

In order to investigate the cross-coupling phenomenon and to test the correction method presented in subsection 2.1, two piezoelectric transducer arrays are fabricated (Fig. 1).

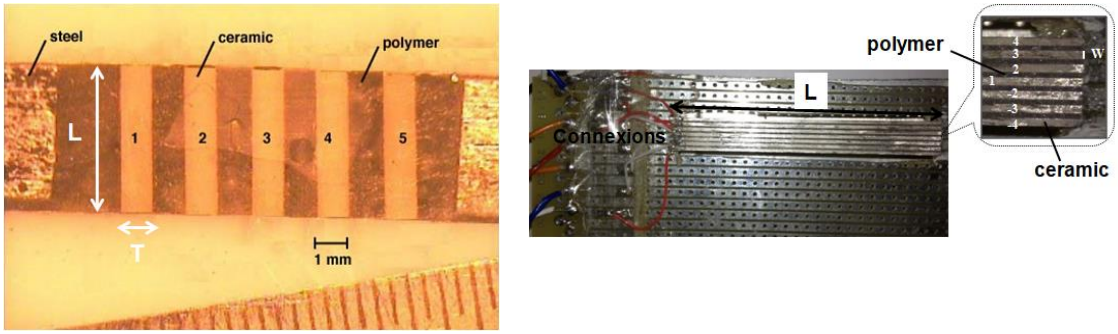

(a) Five-element transducer array (b) Seven-element transducer array

Fig. 1 Fabricated piezoelectric transducer arrays

In both arrays, the piezoelectric elements are polarized along their thickness T, i.e. the electric field is applied in the thickness direction. The first prototype is composed of five elements having a thickness T=1 mm, a width W=3 mm and a length L=4.5 mm. Whereas the second one is composed of seven elements having the dimensions T=3.3 mm, W=0.7 mm, and L=37 mm. The piezoelectric elements utilized for both prototypes (five-element and seven-element transducer arrays) are made of PZ27 material (Ferroperm piezoelectric ceramic). The polymers used to fill the kerfs between the elements are respectively an epoxy resin for the first array and an Acrylic PLEXCIL resin for the second one. Concerning the five-element array, two parts of steel are bonded on each side in order to facilitate its handling. All material properties are listed in Table 1. It is important to precise that the dependence of the polymer's viscoelastic properties (Young Modulus) on the frequency is not considered in this study.

In order to obtain the most efficient conversion of the electrical energy into a mechanical one, we choose to excite each transducer at its natural resonant frequency. As the purpose is also to favor the normal displacement at the surface of the array elements, it leads naturally to the choice of transverse vibration resonance for the first prototype (five-element array) and thickness vibration resonance for the second one (seven-element array). The corresponding resonance frequencies can be calculated using the Eqs. (4-5) [12]:

$$F_{r5} = \frac{N_w}{W} \tag{4}$$

$$F_{r7} = \frac{N_t}{T} \tag{5}$$

where N_i (i corresponds to "w" or "t") is the frequency constant equivalent to the product of the resonance frequency and the dimension governing this latter. N_i is also equal to half the sound velocity in the same direction.

Table 1 Properties of PZ27, steel, and polymers [25]

PZ 27 ceramic		Polymer 1 Epoxy		Polymer 2 Acrylic PLEXCIL		Steel	
$S_{11}^E(10^{-12}\ Pa^{-1})$	17	Young Modulus E(GPa)	2.5	Young Modulus E(GPa)	5.64	Young Modulus E(GPa)	210
$S_{12}^E(10^{-12}\ Pa^{-1})$	-6.71						
$S_{13}^E(10^{-12}\ Pa^{-1})$	-8.53						
$S_{33}^E(10^{-12}\ Pa^{-1})$	23						
$S_{44}^E(10^{-12}\ Pa^{-1})$	43.47	Poisson ratio μ	0.36	Poisson ratio μ	0.329	Poisson ratio μ	0.33
$S_{66}^E(10^{-12}\ Pa^{-1})$	47.42						
d_{15} (pC/N)	500						
d_{31} (pC/N)	-170						
d_{33} (pC/N)	425	Density $\rho(kg/m^3)$	1100	Density $\rho(kg/m^3)$	1175	Density $\rho(kg/m^3)$	7800
$\varepsilon_{11}^S/\varepsilon_0$	1130						
$\varepsilon_{33}^S/\varepsilon_0$	914						
$\rho(kg/m^3)$	7700						

3. Numerical Study of Cross-Coupling

3.1. Cross-coupling effects

To study the influence of the acoustical interactions in water (propagation medium in medical imaging applications) and the mechanical interactions due to the filling material on the performances of an element in a piezoelectric transducer array (the Transmitting Voltage Response (TVR), the surface displacement profile and the directivity pattern), the structure in Fig. 2 is modeled using Finite Elements Model (FEM) composed of isoparametric quadratic elements and using the ATILA code. This structure is composed of seventeen piezoelectric elements made of PZ27 ceramic bounded to each other by Acrylic PLEXCIL resin (filling material). The spacing between the elements (d) is chosen equal to 1.2 mm in order to respect the Nyquist criterion and to avoid grating lobes. Each element of the studied array has a thickness T=3.3 mm, a width W=0.7 mm and its length are chosen to be 37 mm long, with a Length-to-Thickness Ratio (L/T) of about 11.21, thus this length can be considered as infinite and a plane strain approximation assumed. The transducer array radiates in a fluid medium (water in medical imaging applications) meshed with isoparametric quadratic elements respecting the λ/4 criterion. This medium is limited by a non-reflecting surface Γ_e made up of dipolar elements that absorb the outgoing acoustic wave almost completely. Furthermore, only half the domain is meshed due to symmetry.

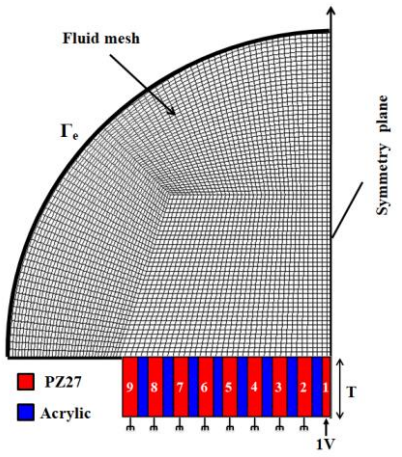

Fig. 2 Schematic description of a seventeen-element transducer array radiating in water

Firstly, in order to consider interactions between elements, the central element "1" is excited while the others are grounded. The filling material (Acrylic PLEXCIL) is assumed to have low mechanical losses (loss factor tanδ=E' / E=5 %; E

and E' are the real and the imaginary parts of Young Modulus). The calculation of the surface displacement at the resonance frequency 443 kHz (maximum of TVR) is shown in Fig. 3.

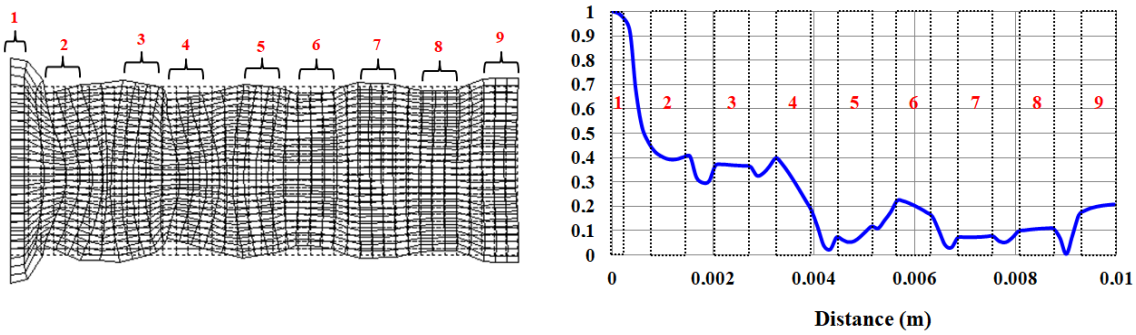

(a) Displacement field (b) Normalized displacement amplitude

Fig. 3 Seventeen element transducer array: displacement field and normalized amplitude

This figure indicates that the excited element "1" vibrates in thickness mode and that parasitic displacements due to cross-coupling phenomenon are observed on the neighboring elements (2, 3,…9). It can be noticed from these results that important parasitic displacements are obtained particularly on the third neighboring elements 2, 3, and 4 (normalized displacement amplitudes about 0.4, 0.38, and 0.3). For this reason, it is decided in this paper to study transducer arrays composed of five and seven elements.

In order to evaluate the effects of the filling material Loss Factor (LF=tanδ) on the transducer array performances (TVR, directivity pattern and displacement), the thickness resonant frequency is first determined by computing the TVR of five transducer arrays with different values of LF: 2%, 7%, 11%, 15%, and 20%. In reality, the loss factor tanδ=E' / E depends on the operating frequency. Nevertheless, in order to simplify the study, this dependence is not considered in our case. Consequently, the value of LF is assumed constant in the band frequency 300 kHz-600 kHz. The results obtained in this situation are given in Fig. 4. According to this figure, the resonant frequency F_r (maximum of TVR) is obtained at 443 kHz for all cases. It is also clear that the filling material with the highest LF reduces strongly the parasitic vibrations (particularly around the frequencies 335 kHz, 385 kHz, 415 kHz, and 770 kHz) at the expense of the TVR level which decreases as long as the LF of the filling material increases.

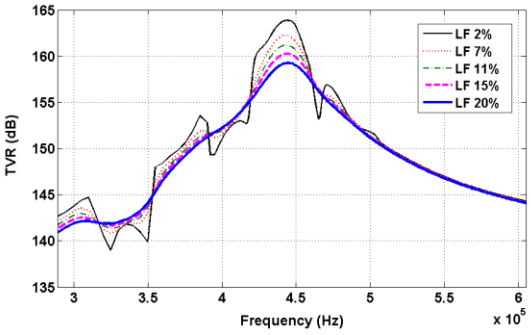

Fig. 4 TVR of transducer arrays filled with resins having loss factors 2%, 7%, 11%, 15%, and 20%

In order to show the influence of the LF on the directivity pattern of the transducer array and to choose the optimum value of the loss factor, the results obtained in the case of LF values 2%, 11%, 15%, 20%, 30%, and 40% are compared in Fig. 5.

Firstly, it can be noticed that the directivity patterns are not omnidirectional (dashed curve) as in the case of a single element (reference case) but they present a main lobe in the direction 0° and other undesirable side lobes are obtained in the directions 20°, 43°, and 80°. This is due to the cross-coupling phenomenon which modifies the directivity pattern especially in the case of transducer arrays with a lossless filling material ($\tan(\delta) \leq 15\%$). This result allows concluding that as long as the LF increases the secondary lobes disappear and the cross-coupling decreases significantly. It can also be noticed that starting from

a loss factor 15%, the directivity pattern remains approximately unchanged. Thus, theoretically, this value of LF can be considered as an optimum value of loss factor.

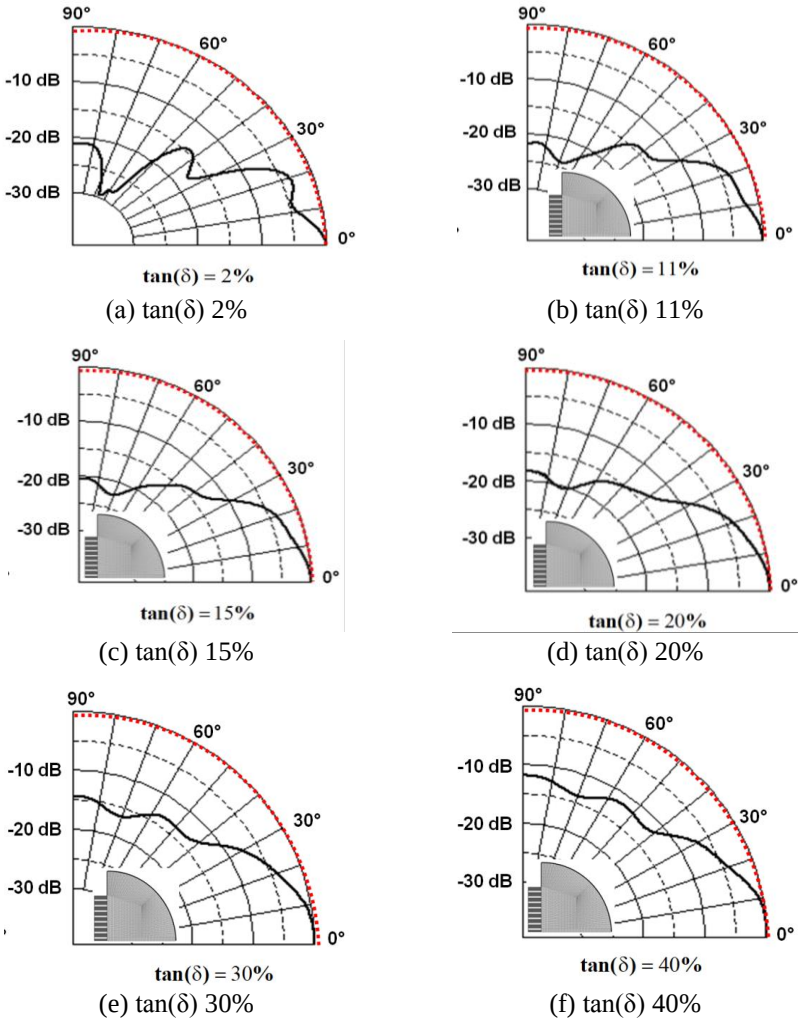

(a) tan(δ) 2% (b) tan(δ) 11%

(c) tan(δ) 15% (d) tan(δ) 20%

(e) tan(δ) 30% (f) tan(δ) 40%

Fig. 5 Directivity pattern of some values of LF (solid line) compared to the single elements' one (dashed line)

Fig. 6 confirms the previous result by comparing the normalized displacement amplitudes computed at the radiating surface of five transducer arrays with different filling material loss factors 2%, 7%, 11%, 15%, and 20%. It can be noticed that the displacement on the neighboring elements "2," "4," "6," and "9" decreases rapidly in the case of high loss factors, e.g. 20%. Whereas, a weak reduction of displacement is observed on the elements "3" "5," "7," and "8." In addition to this, it is important to notice that the displacement (speed) on the excited element "1" is also reduced as mentioned by Stytsenko [34]. Nevertheless, this reduction is weak compared to that of the parasitic displacements, particularly in the case of the elements "2," "4," "6," and "9." This result is not visible in Fig. 6 because it displays the normalized displacement amplitudes.

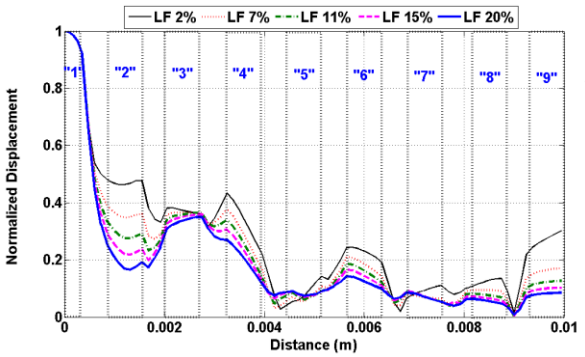

Fig. 6 Normalized displacement amplitude of some values of filling material LF 2%, 7%, 11%, 15%, and 20%

Finally, it can be concluded from this study, that filling materials with high LF can be one of the solutions which contributes to the reduction of cross-coupling phenomenon.

3.2. Cross-coupling correction

In our case, calculations carried out previously on a seventeen-element array demonstrated that only the elements nearest the excited one contribute to cross-coupling. For this reason, it is decided to test the cross-coupling correction method in the case of the seven-element array presented previously in subsection 2.2 (Thickness * Width * Length=3.3 * 0.7 * 37 mm^3). The length L is firstly considered as infinite (because L/T ≈ 11.21 and L/W ≈ 52.5), thus a plane strain approximation is assumed (the normal displacement along the length of the elements is considered uniform) and 2D-FEM is utilized to check the validity of the correction method. In the second time, 3D-FEM considering the length of the elements is used in order to test the correction method in real conditions, i.e. the normal displacement along the length of the elements is not necessarily uniform.

(1) 2D Finite Elements Model

In this subsection, the seven element transducer array is modeled using 2D FE Model similar to the one of the seventeen-element array (subsection 3.1). In order to consider interactions between elements, the central element "1" is driven by an electrical voltage 1V while its neighboring elements are grounded (Fig. 7).

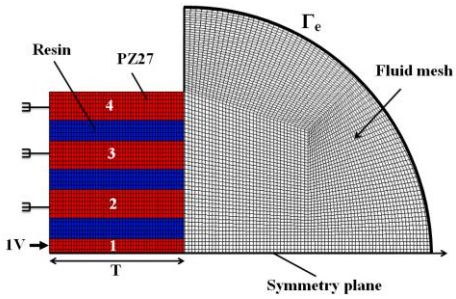

Fig. 7 Schematic description of a seven-element transducer array radiating in water

Fig. 8 displays the displacement field and the far-field directivity pattern computed at the thickness resonant frequency 454 kHz. It is clearly observed from Fig 8(a) that the excited element "1" vibrates in thickness mode, and that parasitic displacements due to cross-coupling phenomenon are observed on the neighboring elements "2," "3," and "4" (normalized displacement amplitudes about 0.42, 0.39, and 0.61). The amplitude of the displacement on the element "4" is about half that obtained on the excited element "1." Consequently, this result denotes the importance of edge effects.

The parasitic displacements disturb the far-field directivity pattern of the excited element as seen in Fig. 8(b). Firstly, it can be noted that the directivity pattern presents the main lobe in the direction ±20° instead of 0° (axial direction), and secondly, that other side lobe is obtained in the directions ±55° and ±85°. These results indicate clearly that cross-coupling disturbs the performance of the transducer array.

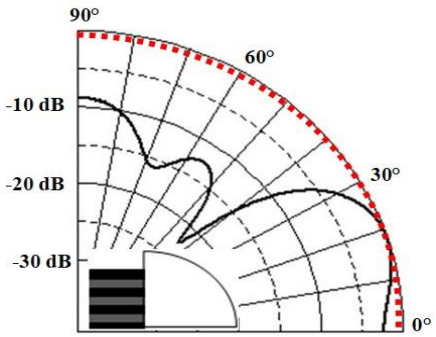

(a) Displacement field

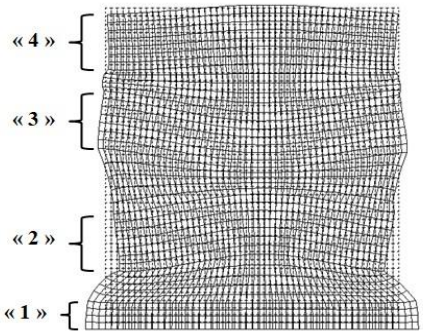

(b) Directivity pattern: transducer array without correction (solid line) and single element (dashed line)

Fig. 8 Numerical displacement field and directivity pattern

In order to reduce this parasitic phenomenon, electrical voltages $A_1^2 = (-0.2 + 0.46j)$, $A_3^1 = (-0.34 + 0.29j)$ and $A_4^1 = (0.25 + 0.27j)$ calculated using the correction method explained previously in section 2.1, are applied to the neighboring elements "2," "3," and "4" respectively. The computed displacement field and directivity pattern are shown in Fig. 9. This latter indicates clearly that the application of electrical voltages to the neighboring elements reduces the parasitic displacements and improves the directivity pattern of the array. Hence the maximum pressure is obtained in the axial direction (near 0°) and the result obtained is similar to that of a single element. Finally, the numerical results demonstrate the ability of the technique to reduce cross-coupling.

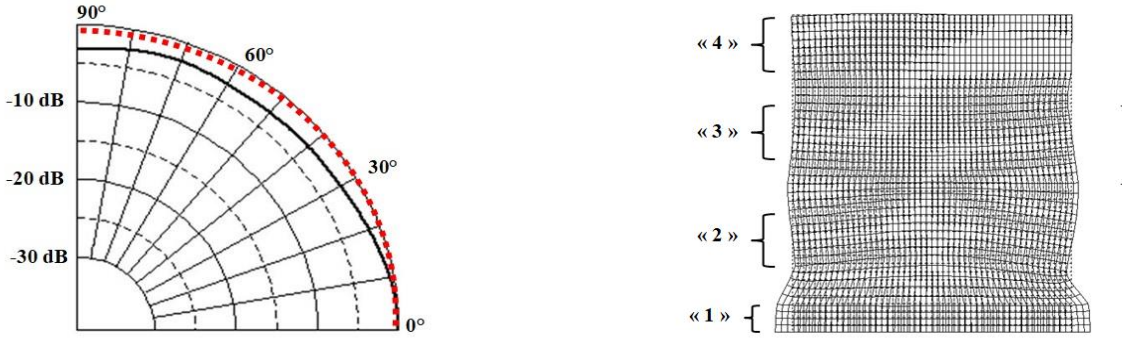

(a) Displacement field

(b) Directivity pattern: transducer array with correction (solid line) and single element (dashed line)

Fig. 9 Numerical displacement field and directivity pattern

(2) 3D Finite Elements Model

In order to test the correction method in real conditions, i.e. considering the length of the transducer array elements a 3D-FE Model composed of isoparametric hexahedral elements is developed using the ATILA code. In this study, only half the domain is meshed due to symmetry. The schematic description of the modeled seven-element array is shown in Fig. 10.

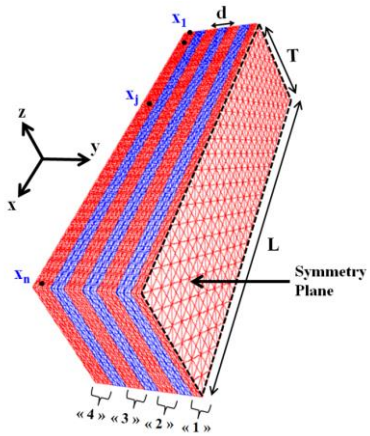

Fig. 10 Schematic description of a seven-element transducer array

Firstly, the central element "1" is excited at its resonant frequency while its neighboring elements "2," "3," and "4" are grounded. Fig. 11(a) displays the normal displacement amplitude in different points xi (Fig. 10) along the length of each element of the transducer array. As expected the numerical results indicate the presence of important parasitic displacements on the passive elements "2," "3," and "4" due to cross-coupling phenomenon. In addition to this, the displacement obtained at the surface of the array elements is not uniform as assumed in 2D-FEM. In this situation, the normal displacement depends on the position x due to the finite length of the elements (L=37 mm). In order to reduce cross-coupling phenomenon, the electrical voltages $A_j^1 = (j = 2,3,4)$ calculated previously in the case of 2D-FEM are applied to the neighboring elements "2," "3," and "4" respectively. Fig. 11(b) represents the normal displacement amplitudes obtained at the surface of the transducer array

elements. The comparison of the results obtained before and after cross-coupling correction indicates the ability of the method to reduce the parasitic displacements even when the normal displacement along the length of the array elements is not uniform. It can also be observed in Fig. 11(b) that the amplitude of the excited element is also reduced, but remains superior to that of the parasitic displacements. This reduction is due to the minimization of the parasitic displacements contribution to the total displacement obtained on the excited element "1." Consequently, the minimization of the cross-coupling improves the directivity pattern of the transducer array at the expense of the TVR level which is reduced.

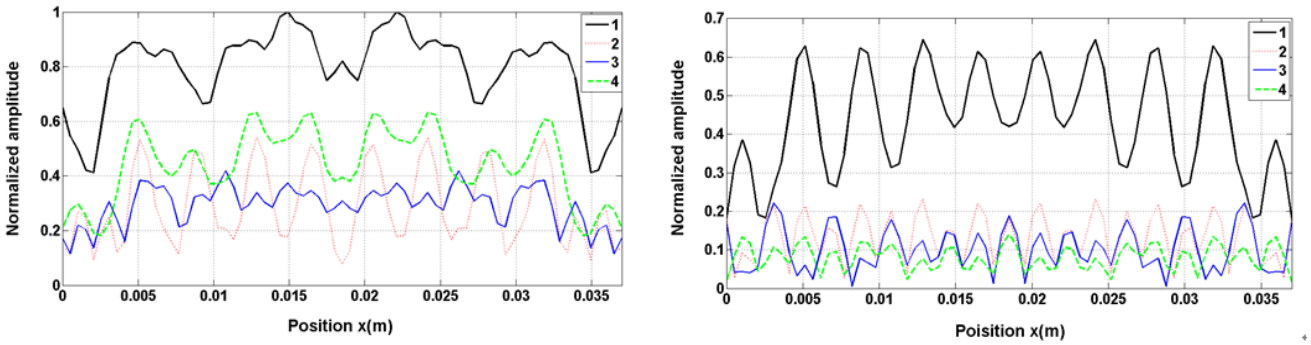

(a) Without cross-coupling correction (b) With cross-coupling correction

Fig. 11 Normalized displacement amplitude at the surface of the array elements

4. Experimental Results

In this section, the cross-coupling correction method is tested experimentally on the fabricated transducer arrays: five-element array vibrating in transverse mode and seven-element array vibrating in thickness mode (details are given in subsection 2.2). The proposed experimental setup to measure the displacement at the surface of the transducer arrays is composed of low-frequency generators (Agilent 33250A) used to excite the array elements around their resonance frequency. Displacement at different points on the array is achieved using a Polytech psv400 laser vibrometer controlled by a computer.

4.1. Five-element transducer array

The cross-coupling correction method is first tested in the case of the five-element transducer array described in subsection 2.2 (T*W*L=1*3*4.5 mm^3). Foremost, in order to consider, the interactions between the array elements (cross-coupling), the central element "3" is excited at its resonant frequency 235 kHz while its neighboring elements are grounded. The normal displacement measured in the middle of the transducer array elements ("1," "2," "3," "4," and "5") is compared to the numerical result obtained using FE as shown in Fig. 12. First, a good agreement is observed between measurement and simulations. Second, parasitic displacements are obtained on the neighboring elements "1," "2," "4," and "5". This result corresponds to the cross-coupling phenomenon which should be reduced.

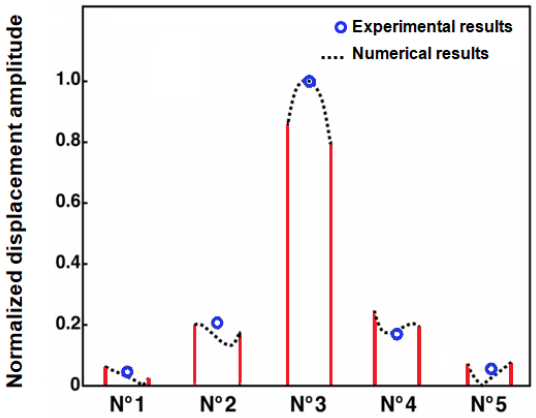

Fig. 12 Normalized displacement amplitude obtained on each element of the transducer array before cross-coupling correction

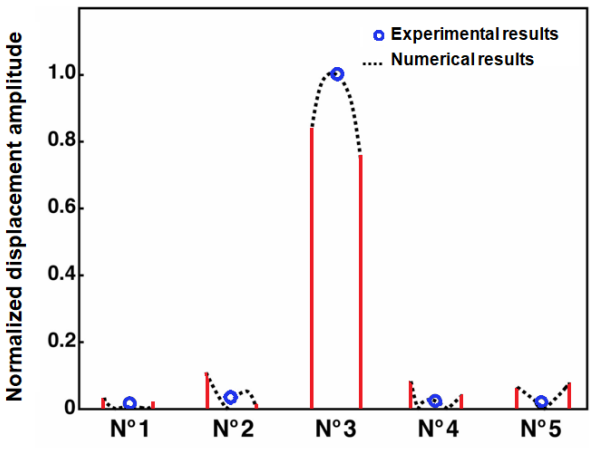

Fig. 13 Normalized displacement amplitude obtained on each element of the transducer array after cross-coupling correction

In order to reduce cross-coupling phenomenon, electrical voltages $A_j^3 = (j = 1,2,4,5)$ calculated using the correction method described in subsection 2.1 are applied to the neighboring elements "1," "2," "4," and "5" respectively. The normal displacement amplitude measured on the transducer array elements ("1," "2," "3," "4," and "5") is compared to the numerical one as shown in Fig. 13. This latter indicates a good agreement between simulation and experiment. In addition to this, the comparison of the results obtained before (Fig. 12) and after cross-coupling correction (Fig. 13) demonstrates clearly the ability of the method to reduce the parasitic displacements, i.e. cross-coupling.

4.2. Seven-element transducer array

The seven-element transducer array described previously in subsection 2.2, i.e. having the dimensions T * W* L = 3.3 * 0.7 * 37 mm^3 and vibrating in thickness mode is also characterized experimentally by electrical and mechanical measurements. Firstly, electrical impedance measurements are realized on the transducer array elements ("1," "±2," "±3," and "±4") in order to check the quality of the fabrication process (symmetry of the transducer array) and to show the presence of cross-coupling in this kind of transducer arrays. In this study, the elements "1," "±2," "±3," and "±4" correspond respectively to the central element (the element situated in the middle of the transducer array) and its first, second and third neighboring elements. Each element is connected to an impedance analyzer while its neighboring elements are connected to the ground by 50 Ω resistors.

Fig. 14 compares the electrical impedance curves obtained with that of a single piezoelectric element having the same dimensions. After analysis, different conclusions can be made. Firstly, in both cases (single element and transducer array elements), it can be easily observed the presence of two thickness modes: a fundamental thickness mode around the frequency F_r = 500 kHz and it's harmonic around the frequency F_r = 1.55 MHz. A frequency shift can also be seen between the resonance (minimum of electrical impedance) and anti-resonance (maximum of electrical impedance) frequencies, obtained in the case of a single element (element isolated from the others) and the result measured when the element is bounded to the others. Therefore, the presence of neighboring piezoelectric elements shifts the thickness resonance and anti-resonance frequencies to higher ones. In addition to this, the magnitude of electrical impedance measured on the array elements "1," "±2," "±3," and "±4" is lower than that measured of the single element. This result is due to acrylic resin utilized to attach the transducer array elements to each other. This filling material introduces mechanical losses which decrease the impedance magnitude. From Fig. 14 (b) it can be observed that the electrical impedance curves of the elements "2" and "-2", "3" and "-3", "4" and "-4" are similar, which indicates a good symmetry of the elements and validates the fabrication process. From the same figure, it can be seen that the resonance frequency (minimum of electrical impedance) can be easily distinguished in the case of the single element (F_r = 454 kHz). Whereas, in the case of the transducer array elements "1," "±2," "±3," and "±4" several parasitic vibrations are obtained around this frequency making it difficult to distinguish. These parasitic vibrations correspond to cross-coupling (undesired interactions between the array elements), which change the individual element electromechanical

behavior and thus decreases the transducer array performance. Finally, the comparison of the electrical impedance curves of the elements "1," "±2," "±3," and "±4" shows a frequency shift between the anti-resonance frequencies. In this situation, the elements away from the central one "1" tend to have the same anti-resonance frequency than that of the single element.

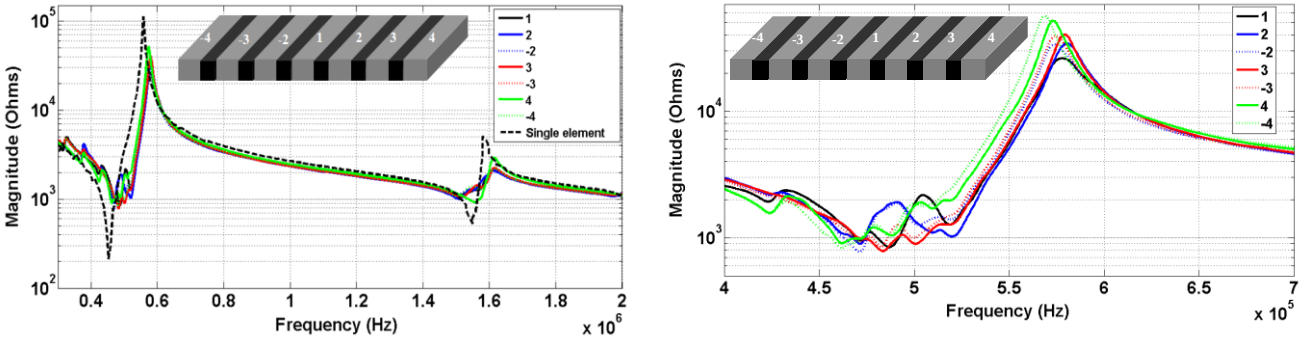

(a) Thickness resonant mode and it's harmonic (b) Thickness resonant mode

Fig. 14 Electrical impedance magnitude measured on the transducer array elements "1," "±2," "±3," and "±4"

In order to evaluate the cross-coupling effects, displacement at different points on the transducer array is achieved using a Polytech psv400 laser vibrometer controlled by a computer. Figure 15 shows the displacement measured at the surface of the transducer array when the central element "1" is excited by a sinusoidal signal having a frequency 481 kHz (thickness resonance frequency) and a magnitude 1V, and its neighboring elements grounded. It is clearly observed from this figure that the driven element vibrates mainly in thickness mode, but the displacement is not completely the same in all points, particularly near the edges. Furthermore, the cross-coupling phenomenon is observed by the presence of parasitic displacements on the passive elements, i.e. elements "±2," "±3," and "±4". In addition to this, due to the limited number of elements in the transducer array (seven elements), the parasitic displacement measured on the third elements "±4" is significant compared to the one obtained on the elements "±2" and "±3." In other words, the edge effects are not negligible.

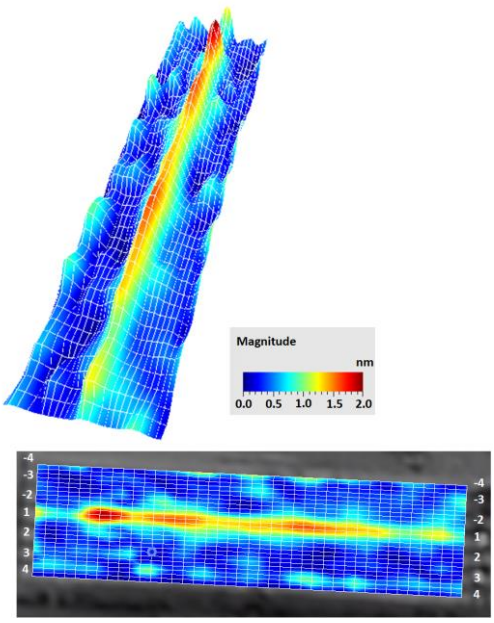

Fig. 15 Displacement measured at the surface of the transducer array at the resonance frequency 481 kHz

In order to check the validity of the 3D-FEM introduced in subsection 2.3, the normal displacement computed in different points xi (Fig. 10) along the length of the excited element "1" and its first neighboring element "2" is compared to the measured one in Fig. 16. First of all, a good agreement is obtained between numerical and experimental results. As expected both of them to show a dominant thickness mode (important displacement on the excited element "1"), and significant parasitic displacements on the passive elements "2" and "-2." In addition to this, the displacement at the surface of the elements is not

uniform due to the finite length of the elements (L=37 mm). Furthermore, some differences are observed between the displacement measured at the surface of the first neighboring elements “2” and “-2” due to small defects in the fabricated transducer array (small dissymmetry).

Finally, in order to reduce cross-coupling phenomenon, electrical voltages calculated using the correction method are applied to the neighboring elements. In order to avoid edge effects, which are significant in our case, the study is limited to the first “±2” and second “±3” neighboring elements. The third neighboring elements “±4” remain connected to the ground. The normal displacement amplitude measured in the middle of the transducer array elements before and after cross-coupling correction is compared in Fig. 17. It is clearly observed that the parasitic displacements on the neighboring elements have been reduced significantly by applying the correction voltages, which demonstrates the ability of the correction method to reduce cross-coupling phenomenon (more details can be found in our previous work [16]).

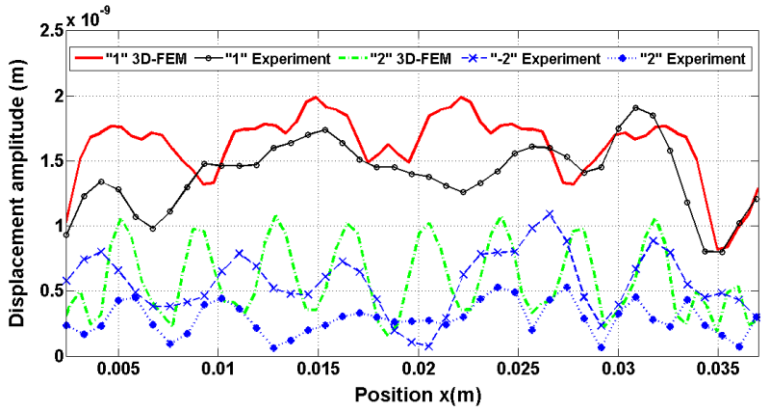

Fig. 16 Displacement amplitude obtained on the elements “1,” “2,” and “-2”

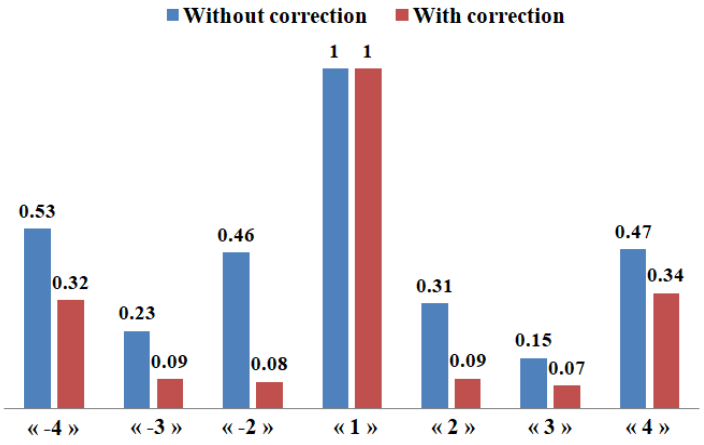

Fig. 17 Normalized displacement amplitude in the middle of the array

5. Conclusions

In this paper, cross-coupling in piezoelectric transducer arrays is analyzed numerically using 2D and 3D Finite Elements Models and experimentally by electrical impedance and displacement measurements. Firstly, the influence of the filling material losses on the performance of a seventeen-element transducer array is studied. Secondly, in order to minimize cross-coupling in the studied transducer arrays, the correction method performed previously in the case of the transducer arrays vibrating in thickness mode, is tested using 3D-FEM considering the real length of the transducer array. The proposed technique is then extended to a transducer array vibrating in transverse mode. The results obtained have shown that a filling material with a high loss factor ($\tan\delta \geq 15\%$) contributes significantly to the reduction of cross-coupling. The ability of the correction method to reduce cross-coupling is also demonstrated even when the displacement at the radiating surface of the transducer arrays is not uniform.

Conflicts of Interest

The authors declare no conflict of interest.

References

[1] J. Y. Zhang, W. J. Xu, J. Carlier, X. M. Ji, S. Queste, B. Nongaillard, and Y. P. Huang, "Numerical and experimental investigation of kerf depth effect on high-frequency phased array transducer," Ultrasonics, vol. 52, no. 2, pp. 223-229, February 2012.

[2] Q. Yue, D. Liu, J. Deng, X. Zhao, D. Lin, W. Di, X. Li, W. Wang, X. Wang, and H. Luo, "Design and fabrication of relaxor-ferroelectric single crystal PIN-PMN-PT/epoxy 2-2 composite based array transducer," Sensors and Actuators A: Physical, vol. 234, pp. 34-42, October 2015.

[3] A. Bezanson, R. Adamson, and J. A. Brown, "Fabrication and performance of a miniaturized 64-element high-frequency endoscopic phased array," IEEE Transactions on Ultrasonics, Ferroelectrics, and Frequency Control, vol. 61, no. 1, pp. 33-43, January 2014.

[4] Z. Zhang, J. Xu, L. Yang, S. Liu, J. Xiao, X. Li, X. Wang, and H. Luo, "Design and comparison of PMN-PT single crystals and PZT ceramics based medical phased array ultrasonic transducer," Sensors and Actuators A: Physical, vol. 283, pp. 273-281, November 2018.

[5] C. Liu, F. T. Djuth, Q. Zhou, and K. K. Shung, "Micromachining techniques in developing high-frequency piezoelectric composite ultrasonic array transducers," IEEE Transactions on Ultrasonics, Ferroelectrics, and Frequency Control, vol. 60, no. 12, pp. 2615-2625, July 2013.

[6] J. M. Cannata, J. A. Williams, Q. Zhou, T. A. Ritter, and K. K. Shung, "Development of a 35-MHz piezo-composite ultrasound array for medical imaging," IEEE Transactions on Ultrasonics, Ferroelectrics, and Frequency Control, vol. 53, no. 1, pp. 224-236, January 2006.

[7] H. R. Chabok, J. M. Cannata, H. H. Kim, J. Williams, J. Park, and K. K. Shung, "A high-frequency annular-array transducer using an interdigital bonded 1-3 composite," IEEE Transactions on Ultrasonics, Ferroelectrics, and Frequency Control, vol. 58, no. 1, pp. 206-214, January 2011

[8] Q. Zhian, P. A. Lewin, and P. E. Bloomfield, "Variable-frequency multilayer PVDF transducers for ultrasound imaging," Proc. SPIE, April 1997, vol. 3037, pp. 2-12.

[9] B. T. Khuri-Yakub and O. Oralkan, "Capacitive micromachined ultrasonic transducers for medical imaging and therapy," Journal of Micromechanics and Microengineering, vol. 21, no. 5, pp. 54004-54014, May 2011.

[10] J. Assaad and C. Bruneel, "Radiation from finite phased and focused linear array including interaction," The Journal of the Acoustical Society of America, vol. 101, no. 4, pp. 1859-1867, 1997.

[11] Y. Roh and M. S. Afzal, "Optimal design of a sparse planar array transducer for underwater vehicles by inclusion of crosstalk effect," Japanese Journal of Applied Physics, vol. 57, no. 7S1, pp. 07LG02-1-07LG02-7, June 2018.

[12] M. Celmer and K. J. Opielinski, "Research and modeling of mechanical crosstalk in linear arrays of ultrasonic transducers," Archives of Acoustics, vol. 41, no. 3, pp. 599-612, 2016.

[13] M. Celmer, K. J. Opielinski, and M. Dopierała, "Structural model of standard ultrasonic transducer array developed for FEM analysis of mechanical crosstalk," Ultrasonics, vol. 83, pp. 114-119, February 2018.

[14] S. Ballandras, P. F. Edoa, F. Langrognet, W. Steichen, and G. Pierre, "Prediction and measurement of cross-talk effects in a periodic linear array built using ultrasound micromachining," Proc. IEEE Ultrasonics Symposium, October 2000, pp. 1139-1142.

[15] K. J. Opielinski, M. Celmer, and R. Bolejko, "Crosstalk effect in medical ultrasound tomography imaging," Joint Conference-Acoustics, September 2018, pp. 1-6.

[16] A. Bybi, S. Grondel, J. Assaad, A. C. Hladky-Hennion, C. Granger, and M. Rguiti, "Reducing crosstalk in array structures by controlling the excitation voltage of individual elements: a feasibility study," Ultrasonics, vol. 53, no. 6, pp. 1135-1140, August 2013.

[17] S. Pyo and Y. Roh, "Analysis of the crosstalk in an underwater planar array transducer by the equivalent circuit method," Japanese Journal of Applied Physics, vol. 56, no. 7S1, pp. 07JG01-1-07JG01-6, June 2017.

[18] F. P. Branca, F. Bini, F. Marinozzi, and A. Grandoni, "Optimum choice of acoustic properties of filling materials using optical measurement," IEEE Ultrasonics Symposium (IUS), August 2004, vol. 3, pp. 1663-1665.

[19] W. Lee and Y. Roh, "Optimal design of a piezoelectric 2D array transducer to minimize the cross-talk between active elements," IEEE Ultrasonics Symposium (IUS), September 2009, pp. 2738-2741.

[20] H. J. Fang, Y. Chen, C. M. Wong, W. B. Qiu, H. L. Chan, J. Y. Dai, Q. Li, and Q. F. Yan, "Anodic aluminum oxide-epoxy composite acoustic matching layers for ultrasonic transducer application," Ultrasonics, vol. 70, pp. 29-33, August 2016.
[21] M. H. Amini, T. W. Coyle, and T. Sinclair, "Porous ceramics as backing element for high-temperature transducers," IEEE Transactions on Ultrasonics, Ferroelectrics, and Frequency Control, vol. 62, no. 2, pp. 360-372, February 2015.
[22] S. M. Ji, J. H. Sung, C. Y. Park, and J. S. Jeong, "Phase-canceled backing structure for lightweight ultrasonic transducer," Sensors and Actuators A: Physical, vol. 260, pp. 161-168, 2017.
[23] J. Henneberg, A. Gerlach, H. Storck, H. Cebulla, and S. Marburg, "Reducing mechanical cross-coupling in phased array transducers using stop band material as backing," Journal of Sound and Vibration, vol. 424, pp. 352-364, 2018.
[24] B. Cugnet, A. C. Hladky, and J. Assaad, "Numerical cross-coupling in acoustical arrays," Ultrasonics, vol. 40, no. 1-8, pp. 503-506, May 2002.
[25] A. Bybi, C. Granger, S. Grondel, A. C. Hladky-Hennion, and J. Assaad, "Electrical method for crosstalk cancellation in transducer arrays," NDT&E International, vol. 62, pp. 115-121, March 2014.
[26] S. Zhou, G. L. Wojcik, and J. A. Hossack, "An approach for reducing adjacent element crosstalk in ultrasound arrays," IEEE Transactions on Ultrasonics, Ferroelectrics, and Frequency Control, vol. 50, no. 12, pp. 1752-1761, December 2003.
[27] P. L. Van Neer, G. Matte, J. Sijl, J. M. Borsboom, and N. de Jong, "Transfer functions of US transducers for harmonic imaging and bubble responses," Ultrasonics, vol. 46, no. 4, pp. 336-340, November 2007.
[28] K. C. T. Nguyen, L. H. Le, M. D. Sacchi, L. Q. Huynh, and E. Lou, "Adaptive noise cancellation in the intercept times-slowness domain for eliminating ultrasonic crosstalk in a transducer array," Proc. IFMBE, 5th International Conference on Biomedical Engineering in Vietnam, Springer, August 2015, vol. 46, pp. 32-35.
[29] C. Ishihara, T. Ikedaa, and H. Masuzawaa, "Higher-frame-rate ultrasound imaging with reduced cross-talk by combining a synthetic aperture and spatial coded excitation," Proc. SPIE, Medical Imaging, Ultrasonic Imaging and Tomography, April 2016, vol. 9790, pp. 97901Z-1-97901Z-7.
[30] L. F. Xu, T. C. Yu, X. Feng, C. P. Yang, Y. Chen, W. Chen, and J. Zhou, "Dimension dependence of thickness resonance behavior of piezoelectric fiber composites," Materials Chemistry and Physics, vol. 218, pp. 34-38, October 2018.
[31] B. Ren and C. J. Lissenden, "Modeling guided wave excitation in plates with surface mounted piezoelectric elements: coupled physics and normal mode expansion," Smart Materials and Structures, vol. 27, 045014, 2018.
[32] A. Mohammadabadi and R. Dugnani, "Design and Evaluation of a Novel Low Acoustic Impedance-Based PZT Transducer for Detecting the Near-Surface Defects," International Journal of Engineering and Technology Innovation, vol. 9, no. 3, pp. 196-211, 2019.
[33] V. K. Chillara, E. S. Davis, C. Pantea, and D. N. Sinha, "Ultrasonic Bessel beam generation from radial modes of piezoelectric discs," Ultrasonics, vol. 96, pp. 140-148, July 2019.
[34] E. Stytsenko, M. Meijer, and N. L. Scott, "Cross-coupling control in linear and 2D arrays," Proc. OCEANS-MTS/IEEE Kobe Techno-Oceans (OTO), May 2018.